COUPLED MAGNETIC-THERMAL BEHAVIOUR OF A SINGLE PHASE TRANSFORMER

Georges Houtappel, Johan Driesen, Ronnie Belmans and Kay Hameyer

Katholieke Universiteit Leuven, Dep. EE (ESAT), Div. ELEN
Kardinaal Mercierlaan 94, B-3001 Leuven, BELGIUM
Fax: +32-16-321020; e-mail: johan.driesen@esat.kuleuven.ac.be

Abstract: This paper presents a method to compute the magnetic and thermal finite-element solution of a single phase transformer using a weak coupling algorithm. Therefore a detailed 2D magnetic and a thermal model are generated, which are meshed separately and solved in a cascade algorithm of a static thermal and a time-harmonic magnetic solver. The results are verified by means of extensive measurements and show very good agreement.

1.- INTRODUCTION

In electromagnetic energy converters, the temperature dependence of several material parameters results in a coupling between the magnetic and the thermal fields. The value of the local temperature is important to calculate the exact conductivity of the conductors and the temperature distribution as such is important considering the ageing process of insulation materials. The heat generated, depends on the currents and flux distribution, calculated in the magnetic FEM model. With the development of fast general purpose static and time-harmonic finite-element solvers [1], it is possible to iterate between the magnetic and thermal solution with a weak coupling algorithm. This approach is used to calculate the steady state currents and temperatures in a 6.3 kVA single phase transformer, cooled by natural convection. Therefore, it is necessary to employ a sufficiently detailed thermal model to be able to project all the data required by the magnetic solver.

2.- WEAK COUPLING ALGORITHM

2.1.- Equations to be solved

For the three cases, full load, no-load and short circuit operation, the separate magnetic and thermal problem have to be solved. For the magnetic problem, the classical time-harmonic solution is used, with interpolations along the non-linear magnetisation curve.

$$\vec{\nabla}\cdot\left(\nu(A)\vec{\nabla}A\right) - j\omega\sigma(T)A = -\vec{J}_S(T) \qquad (1)$$

with:

A [Wb/m]	magnetic vector potential
$\vec{J}_S$ [A/m²]	source current density

When k is considered constant in the temperature range assumed, the thermal problem is linear.

$$k\vec{\nabla}^2 T = -q(\vec{\nabla}\times\vec{A}, \vec{J}_S + \vec{J}_e) \qquad (2)$$

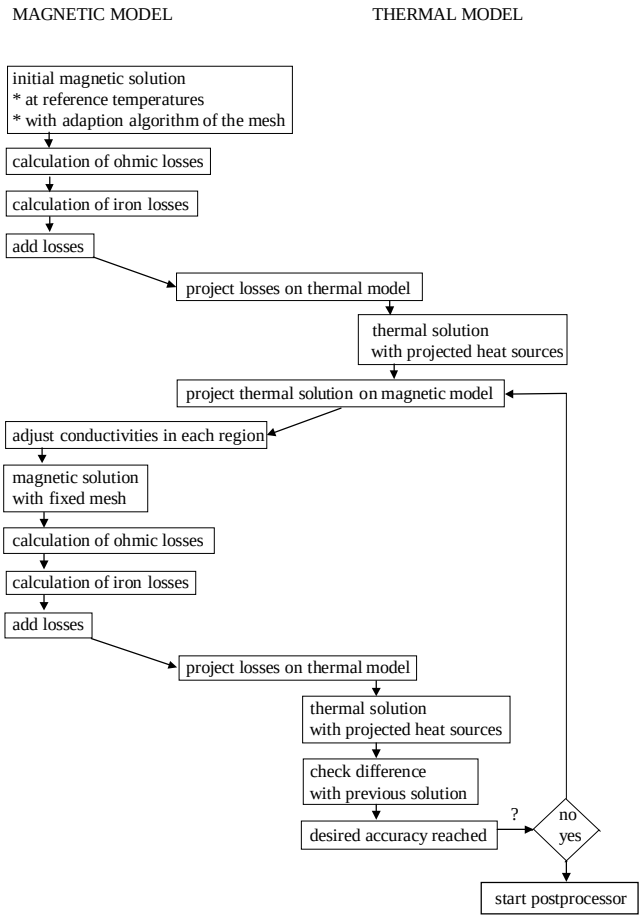

Fig. 1: Flowchart of the cascade coupling algorithm.

with:

q [W/m³]	heat production in a region
k [W/(m.K)]	thermal diffusion coefficient

2.2- Solution Method

In a first step, the magnetic model is solved at a reference temperature (Fig. 1). With this solution, all heat sources (ohmic losses in the coils, magnetic losses in the core) can be evaluated. Since the thermal model does not have the same mesh as the magnetic model, these heat sources are projected on the mesh of the thermal model [1]. In the second step, the thermal model can be solved to obtain the temperature distribution. After another projection of these temperatures on the mesh of the magnetic model, the material properties (conductivities in the coil) can be adjusted to start the new magnetic calculation. Intermediately, appropriate relaxation techniques have to be applied to obtain an acceptable rate of convergence [2].

To become an optimal mesh for each FEM model, the thermal respectively the magnetic one, an adaptation algorithm is used. During the iterations between magnetic and thermal model, these optimal meshes for each model are preserved.

3.-. MAGNETIC MODEL

3.1- Transformer Physical Data

A single phase transformer is used as an example. Table 1 gives some physical properties.

Table 1: Rated electrical data of the transformer

primary voltage	U_{prim}	380	V
primary current	I_{prim}	16.7	A
secondary voltage	U_{sec}	220	V
secondary current	I_{sec}	28.6	A

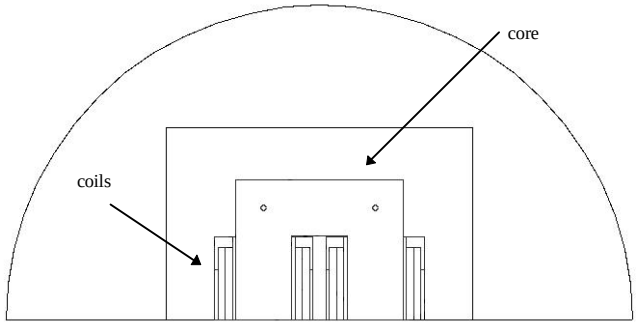

Fig. 2: Geometry of the magnetic model.

transformer ratio	ü	1.727	-
apparent power	S	6300	VA
rated frequency	f	50	Hz

On each leg of the transformer core there are three windings: one with double wound 3 mm wire to form a 110 V winding, a second of 3 mm wire to form a 220 V winding and a third of 1.9 mm thick wire to form a 160 V winding. The 220 V and 160 V winding are put in series with each other and in parallel with the other leg to form the primary voltage. The secondary is the series of the two double wound 110 V windings.

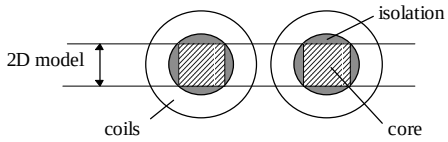

Fig. 3. Horizontal cut through he transformer, showing the position of the 2D model.

3.2- Magnetic Model

Because 2D models are used, the magnetic model is a cut through the core in parallel with the lamination. Although the insulation is not important for the magnetic model, it is modelled because the outline of the magnetic model has to match the outline of the thermal model for the projection algorithm. The bolts holding the core together are modelled, since they are made from magnetic steel. Fig. 2 shows the geometry of the magnetic model.

3.3.- Equivalent materials

Since the leakage inductances were deducted from measurements, the air gap in the core is not modelled in the geometry to reduce the number of nodes. As an alternative, the material for the core is defined using a corrected magnetisation curve. The original M6X magnetisation curve from the manufacturer is corrected for a total air gap length of four mm, considering the core structure [6,7]. The corrected permeability in each point of the magnetisation curve can be calculated using the formula of Hopkinson for non-linear magnetic resistances in the form (3).

$$\theta = \Phi.\frac{l_{Fe}}{S}\frac{\left(1+\frac{l_\delta \mu_{Fe}}{l_{Fe}\mu_0}\right)}{\mu_{Fe}} = \Phi.\frac{l_{Fe}}{S}\frac{1}{\mu_{corr}} \qquad (3)$$

with:

θ [A]	excitation
Φ [Wb]	magnetic flux
l_{Fe} [m]	path length through iron
l_δ [m]	air gap length
S [m²]	section of the core

Fig. 3 shows a horizontal cut through the middle of the transformer, indicating the position of the 2D model. Since this model contains only a small portion of the real coil, the leakage inductances and the resistances have to be corrected.

The leakage inductances of the different windings can be deducted from a short circuit test. Since they are not temperature dependent, they are added in the external circuit equations which describe the different interconnections of the parts of the model representing the coil. The corrections on the resistances however are included in the model by scaling the resistivity of the material describing each specific coil region.

4.- THERMAL MODEL

4.1.- Calculation of Convection Coefficients

The transformer is cooled mainly by natural convection. The dimension analysis of the natural convection problem [3] shows that the convection coefficient h is also a function of the difference between the temperature at the wall and the temperature at infinity. This is expressed by the formula

$$Nu_L = f(Gr_L, Pr) \qquad (4)$$

with:

$Nu_L = \frac{h.L}{k}$	Nusselt number based on a characteristic length L
h [W/(m².K)]	convection coefficient
k [W/(m.K)]	thermal diffusion coefficient
Pr	Prandtl number

The temperature dependence is introduced through the Grashof number which is defined as (5).

$$Gr_L = \frac{g.\beta.\Delta T.L^3}{\nu^2} \qquad (5)$$

with:

g [m/s²]	gravitational acceleration
$\beta = \frac{1}{\mathrm{v}}\frac{\partial \nu}{\partial \mathrm{T}}\Big\|_p$ [K^{-1}]	thermal expansion coefficient of the surrounding air (with v the specific volume). For ideal gasses β=1/T.
$\Delta T = \|T_w - T_\infty\|$ [K]	temperature difference between the wall and the air at infinity
L [m]	characteristic length, in this case the height of the vertical wall
ν [m²/s]	cinematic viscosity

During calculations, the Rayleigh number is frequently used (6).

$$Ra_L = Gr_L \cdot Pr \qquad (6)$$

To calculate the convection coefficients for the vertical walls, the assumption of an isothermal wall is made, together with a homogeneous laminar natural convection stream along this wall [3]. The mean Nusselt number can then be calculated from the equation of Squire and Eckert (7).

$$\overline{Nu_L} = 0.678\, Ra_L^{1/4} \left(\frac{Pr}{0.952 + Pr} \right)^{1/4} \qquad (7)$$

For the horizontal parts of the transformer, like the top part of the core, the formula of Fujii and Imura [3] is used (8).

$$\overline{Nu_L} = 0.16 Ra_L^{1/3} \quad \text{when } Ra_L < 2\times 10^8 \qquad (8)$$

From the measured temperatures at every part of the transformer, it is clear that radiation effects can be neglected and the coefficients of convection can be calculated.

4.2.- Temperature Measurements

To decide for which parts of the transformer the assumptions of the convection mechanisms apply, the temperature distribution in steady state for full-load, short-circuit and no-load is measured. Two principles of measurement are used. First, ten thermocouples are placed on the transformer, some of them inserted between the windings (Fig. 4).

Secondly, the transformer is photographed in steady

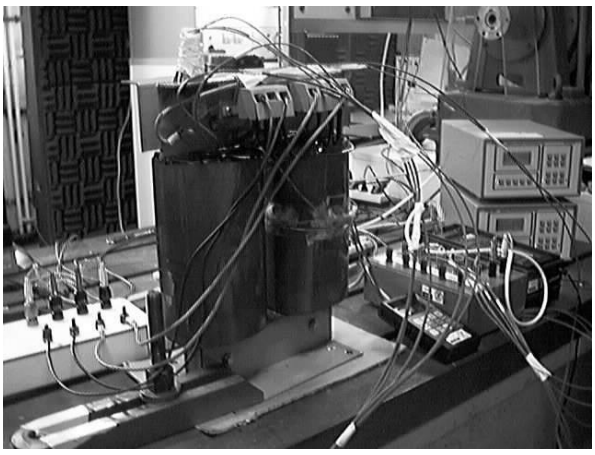

Fig. 4: Transformer with thermocouples and measurement apparatus.

state for the three load types with an infra-red camera. To obtain a homogeneous emittance, one side of the transformer is painted black. With the camera, the temperature distribution can be measured. This is important to make a reliable comparison with the computed results.

4.3- Thermal Model

Except for the boundary conditions, the geometry of the 2D thermal model is the same as in the magnetic model. In the thermal model, the boundaries coincide with the real boundaries of the transformer.

Fig. 5 shows how the windings, together with the insulating materials, are modelled by thermally equivalent regions. Two important 3D problems have to be solved by a correct definition of the equivalent materials in the 2D model.

- As described in the magnetic model, the resistivity of the coil regions is adjusted to represent the whole coil in the 2D model. Therefore, the heat produced in one of the coil regions in the 2D model represents the heat which in reality, is produced along half the circumference of the winding.
- The heat removal from the windings through the core is assumed to flow only in the plane of the 2D model, while in reality, there is a heat flow perpendicular to this plane.

4.4.- Equivalent Materials

For the radial heat flow from the coils to the surrounding air, each sector of the cylindrical coil is considered to be identical. However, for the region where the two legs of the transformer are close together, it can be shown that the hydrodynamic boundary layers of both legs interfere. These effects are however neglected in the thermal 2D model.
Secondly, neglecting the heat flux perpendicular to the plane of the 2D model is adapted because the thermal diffusion in laminated steel is about 20 times smaller than parallel to the lamination [4,5].

Finally, a thermal equivalent model has to be found to represent the thermal behaviour of the coil regions accurately. These regions have to represent the insulated copper wires, together with the layers cardboard, separating each layer of wire from the next layer. The physical properties, used in the calculations, are presented in Table 2.

Table 2: Heat diffusion coefficients for different materials

Material	Heat diffusion coefficient
copper	380 W/(m.K)
resin	0.15 W/(m.K)

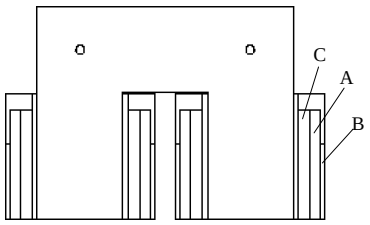

Fig. 5: Geometry of the thermal model used. Three different coil regions are indicated.

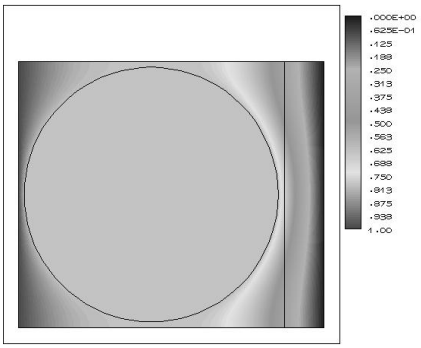

Fig. 6: Solution of the FEM model used to calculate the equivalent thermal properties of one of the copper wires, insulated by resin and separated from the next layer with cardboard.

cardboard	0.14 W/(m.K)

Using these values, the equivalent material properties for each region, with different wire and insulation thickness, is calculated, using a small FEM models (e.g. Fig. 6). The results for the three coil regions are presented in Table 3.

Table 3: Equivalent heat diffusion coefficients for each coil region

Coil region	Symbol	Heat diffusion coefficient
A	k_{eq}^{A}	0.969 W/(m.K)
B	k_{eq}^{B}	0.468 W/(m.K)
C	k_{eq}^{C}	0.695 W/(m.K)

5.- COUPLED CALCULATIONS

5.1.- Calculation of Coupled Phenomena

The effects which need a coupled calculation in this transformer are:

- temperature dependence of the coil resistance
- dependence of ohmic losses in the coils on the currents
- dependence of the iron-losses on the magnetic induction

The first effect can be calculated using (9), which gives for copper the corrected conductance σ, based on the conductance $\sigma_{20°C}$ at 20°C and the temperature in °C.

$$\sigma = \frac{\sigma_{20°C}}{(1+\alpha(T-20°C))} \text{ with } \alpha = 3.9\times10^{-3}\,{}^{1}\!/_{K} \qquad (9)$$

In the coil regions, the dissipated heat is calculated with (10).

$$q = J^2/\sigma \qquad (10)$$

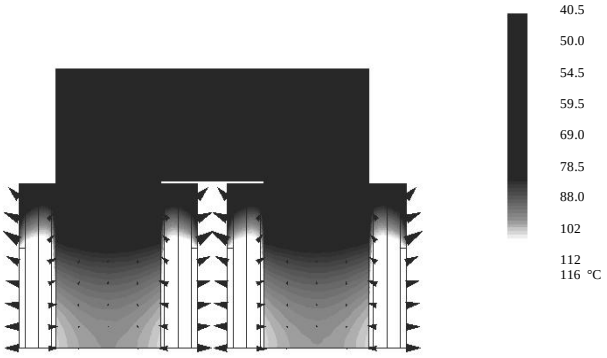

Fig. 7: Calculated temperatures at full load (I_{prim}=16.78 A, I_{sec}=28.85A).

The total iron losses (hysteresis and eddy currents) are calculated using the local values of the induction, the main frequency in the model (50 Hz) and a table, which can be interpolated to give the losses (in W/kg) corresponding to the magnetic induction and the working frequency. The good agreement which is found for the no-load case, shows that this method is sufficiently accurate.

5.2.- Equivalent heat production in stranded conductors

A common technique in modelling electromagnetic energy transducers is the representation of a coil region by an equivalent current carrying region, without modelling each separate conductor. For the magnetic problem, this results in a good approximation. If however, for each element the local heat production is calculated using (10), this result cannot be used in the thermal model directly. With

S_{Cu} [m²] the real copper section,
S_{tot} [m²] the total modelled coil region,
J_{Cu} [A/m²]the current density in the copper,
J_{tot} [A/m²]the current density in the modelled coil region,

the total heat calculated for a coil is (11).

$$\iint_{S_{tot}} \rho_{Cu} J_{tot}^2 \, dS = \rho_{Cu} J_{Cu}^2 \frac{S_{Cu}^2}{S_{tot}} = \rho_{Cu} J_{Cu}^2 S_{Cu} \left(\frac{S_{Cu}}{S_{tot}} \right) \qquad (11)$$

The results of the heat calculation have therefore to be corrected with a filling factor $\left(\frac{S_{tot}}{S_{Cu}}\right)$ to obtain the real heat production in the copper. This is done in a software-routine that calculates the joule losses.

6.- CALCULATION RESULTS AND COMPARISON WITH MEASUREMENTS

6.1.- Full-load

Fig. 7 shows the computed temperature distribution in the thermal model. It is obvious that mainly the coil regions are heated by Joule losses. Vertically seen, the centre of the coils is the most. This is caused by the small outer winding of the thinner wire, which acts like a thermal blanket and as a large heat source. The arrows indicate the direction of heat flow and represent the gradient of the temperature field.

A large portion of the heat is transported towards the outer boundary, where natural convection occurs. The mainly radially directed heat flow in the coil region proves the assumption of homogenous thermal conductivity. Another important part of the heat is transported to the core. Due to vertical up- and downward oriented heat fluxes inside the core, the heat is transported to the top and bottom of the core, were the natural convection provides the cooling. The thin layer of insulating material around the core is a large thermal resistance. At full load, there is a temperature difference of 23°C over this layer. In the centre of the coil, local temperatures of 116°C are possible.

Fig. 8 compares the measurements for which an equivalent point in the model can be found with the measured temperatures. In general, the accuracy obtained is better than 6°C. For point 6, where the deviation is about 10°C, the accuracy of the measurement was much lower, due to practical limitations, such as reachability.

The solution of the circuit equations of the magnetic model has a good accuracy. Table 4 compares the measured electrical parameters, with the calculations.

Table 4: Comparison of measured and calculated electrical parameters

Symbol	Measured	Coupled calculation
I_{prim} [A]	16.76	16.78
I_{sec} [A]	28.76	28.85
P_{prim} [W]	6331	6370
P_{sec} [W]	6082	6149
η [%]	96.1	96.5

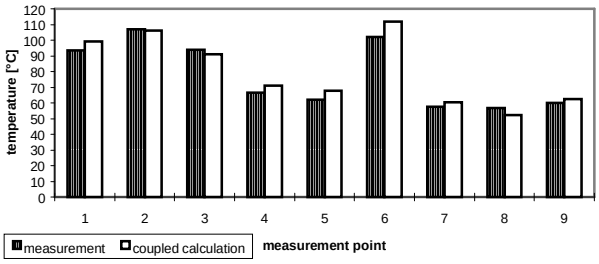

Fig. 8: Comparison of calculated temperatures and measurements.

6.2.- Short circuit and No-load

For the short circuit situation, the accuracy obtained is comparable with the results from the full load case. The only difference is the small amount of heat produced in the core, since the magnetic field is very weak at short circuit operation. This causes the temperatures to be a little bit lower than at full load. The hot spot temperature stays below 90°C for I_{sec}=25.2 A, according to the secondary cold short circuit voltage of 12.1 V.

Similar results were obtained for the no-load case, in which only core losses are significant.

7.- CONCLUSIONS

The results presented here, proof that the cascade magnetic-thermal finite element calculation provides trustful information for the design of a small transformer. The methods for to set up a detailed thermal and magnetic model, including the effects of natural convection and core losses, are hereby validated. The use of two separate models with different meshes makes it possible to optimise the geometry of both the magnetic and thermal model.

Acknowledgement

The authors are grateful to the Belgian "Fonds voor Wetenschappelijk Onderzoek - Vlaanderen" for its financial support of this work and the Belgian Ministry of Scientific Research for granting the IUAP No. P4/20 on Coupled Problems in Electromagnetic Systems. The research Council of the K.U.Leuven supports the basic numerical research. J. Driesen holds a research assistantship of the Belgian "Fonds voor Wetenschappelijk Onderzoek - Vlaanderen".

References

[1] J.Driesen, R.Belmans K.Hameyer,: Adaptive relaxation algorithms for thermo-electromagnetic FEM problems, Proc. 8th Biennial IEEE Conference on Electromagnetic Field Computation, Tuscon-Arizona, USA, 1-3 June 1998, pp.426-430.

[2] R. Mertens, U. Pahner, R. Belmans, K. Hameyer: A Survey of Projection Methods to Improve the Convergence of Non-Linear Problems, Proc. XVth Symp. Electromagnetic Phenomena in Nonlinear Circuits, Liège, Belgium, Sept. 22-24, 1998, pp. 34-37.

[3] J.H. Lienhard, 1981, A Heat Transfer Textbook, New Jersey: Prentice-Hall Inc., 2nd ed..

[4] G. Sobiczewska: Heat conduction parameters for 3D steady state calculations of electrical devices, Proc. of the International Symposium on electromagnetic fields in electrical engineering, Gdansk, Poland, Sept. 1997, pp. 148-151.

[5] A. Williams, Heat flow across stacks of steel laminations", Journal Mech. Eng. Science, vol. 13, no. 3, March 1971.

[6] P.Boer, J.van der Kreek, 1970, Transformatoren, Nijgh & Van Ditmar.

[7] R. Richter: Elektrische Machinen, 1963, Die Transformatoren, Basel: Birkhäuser Verlag, 3rd ed.